

Article

Plasma Surface Engineering to Biofunctionalise Polymers for β -Cell Adhesion

Clara Tran, Nicole Hallahan, Elena Kosobrodova, Jason Tong, Peter Thorn and Marcela Bilek

Special Issue



Plasma Technologies for Surface Engineering

Edited by
Dr. Behnam Akhavan



Article

Plasma Surface Engineering to Biofunctionalise Polymers for β -Cell Adhesion

Clara Tran ^{1,*}, Nicole Hallahan ², Elena Kosobrodova ¹, Jason Tong ² , Peter Thorn ² and Marcela Bilek ¹ 

¹ School of Physics and School of Biomedical Engineering, The University of Sydney, Sydney, NSW 2006, Australia; kosobrodova@fastmail.com.au (E.K.); marcela.bilek@sydney.edu.au (M.B.)

² Charles Perkins Centre, School of Medical Sciences, The University of Sydney, Sydney, NSW 2006, Australia; nic.hallahan@gmail.com (N.H.); jason.tong@rdm.ox.ac.uk (J.T.); p.thorn@sydney.edu.au (P.T.)

* Correspondence: clara.tran@sydney.edu.au

Abstract: Implant devices containing insulin-secreting β -cells hold great promise for the treatment of diabetes. Using in vitro cell culture, long-term function and viability are enhanced when β -cells are cultured with extracellular matrix (ECM) proteins. Here, our goal is to engineer a favorable environment within implant devices, where ECM proteins are stably immobilized on polymer scaffolds, to better support β -cell adhesion. Four different polymer candidates (low-density polyethylene (LDPE), polystyrene (PS), polyethersulfone (PES) and polysulfone (PSU)) were treated using plasma immersion ion implantation (PIII) to enable the covalent attachment of laminin on their surfaces. Surface characterisation analysis shows the increased hydrophilicity, polar groups and radical density on all polymers after the treatment. Among the four polymers, PIII-treated LDPE has the highest water contact angle and the lowest radical density which correlate well with the non-significant protein binding improvement observed after 2 months of storage. The study found that the radical density created by PIII treatment of aromatic polymers was higher than that created by the treatment of aliphatic polymers. The higher radical density significantly improves laminin attachment to aromatic polymers, making them better substrates for β -cell adhesion.

Keywords: beta cells; polymer membrane; plasma immersion ion implantation



Citation: Tran, C.; Hallahan, N.; Kosobrodova, E.; Tong, J.; Thorn, P.; Bilek, M. Plasma Surface Engineering to Biofunctionalise Polymers for β -Cell Adhesion. *Coatings* **2021**, *11*, 1085. <https://doi.org/10.3390/coatings11091085>

Academic Editor: Alenka Vesel

Received: 29 July 2021

Accepted: 6 September 2021

Published: 8 September 2021

Publisher's Note: MDPI stays neutral with regard to jurisdictional claims in published maps and institutional affiliations.



Copyright: © 2021 by the authors. Licensee MDPI, Basel, Switzerland. This article is an open access article distributed under the terms and conditions of the Creative Commons Attribution (CC BY) license (<https://creativecommons.org/licenses/by/4.0/>).

1. Introduction

Microencapsulation of insulin secreting β -cells is a promising approach to treating diabetes. The construction of a microencapsulation device requires that the cells within the implant are protected from immune attack but also that it is permeable to glucose and nutrient inflow as well as insulin outflow. There has been a focus of work on prevention of the foreign body response to an implant and we have recently shown a benefit in coating with IL4 to modify macrophage responses [1]. However, there has been less attention on the internal environment of these devices which, in principle, could be engineered to optimise the support of β -cell function. The approach we favor is the use of an internal polymer scaffold that is bioactivated with extracellular matrices (ECM) proteins that are recognized by β -cells to cause cell adhesion and trigger a range of beneficial cell responses. To this end, we aim to develop methods of stably immobilizing ECM proteins on candidate polymers.

It has long been recognized that β -cells function optimally when situated within their native functional unit—the islets of Langerhans, with the support of ECM. The presence of collagen and laminin has been observed to promote β -cell functions including proliferation, survival, identity, insulin gene expression and protein synthesis, and exocytosis [2,3]. Human β -cells, however, are not known to express or secrete their own ECM proteins and may potentially be dependent on external sources [4,5]. The myriad roles and importance of the native micro-environment in β -cell function as well as current limitations in the islet encapsulation field are the impetus to facilitate reconstruction of a replicating key components of the native micro-environment within synthetic capsules to improve current

β -cell implantation techniques. This includes finding a simple and efficient method to covalently attach ECM proteins onto polymer membranes.

Surface treatment of polymers includes physical and chemical modifications. Chemical modification uses strong chemicals (acid or alkaline) to graft the polymer surface with functional groups [6–8] and is less preferred than the physical approach. Plasma immersion ion implantation (PIII) treatment has been shown to be a robust technique to modify polymers for biomolecule attachment without using linker chemistry or other reagents, eliminating the risk of toxic residues [9]. The continuous bombardment of energetic nitrogen ions onto the polymer surface creates dangling bonds (radicals) which break and recombine as a result of ion implantation. This ion-bombardment induces rearrangement of bonding within the surface, resulting in the formation and removal of volatile groups, leaving a carbonized structure on the surface of polymers [10]. The treatment, occurring not only on the surface but also inside the bulk up to approximately 70 nm underneath the surface [11], sustains the residual unpaired electrons or radicals for months during storage [10]. The stability of radicals in carbonized structure is the greatest difference between the PIII treatment and ultraviolet (UV) radiation treatment in which radicals are formed but are quenched quickly by oxygen in the air to create polar groups on the surface [12,13]. Numerous reports have shown the covalent bonding of biomolecules such as enzymes [14], proteins [15] and oligonucleotides [16] on the PIII-treated polymer surface via the radicals created using this surface activation strategy. In contrast, although the polymer surface after UV radiation is more hydrophilic with the appearance of oxygen containing groups such as aldehyde and carboxylic, protein molecules were only adsorbed on the modified surface [17]. In this work, we proposed the use of PIII treatment on polymers to immobilize laminin, a commonly studied ECM for β -cell attachment, proliferation and insulin secretion [3,18]. The ideal materials for encapsulation need to have a porous structure to facilitate the inflow and outflow of nutrients and insulin, respectively, while protecting β -cells from the immune system. Four polymers, which are commercially available in porous membrane forms that could be used for capsule constructs, were PIII-treated and laminin-functionalized to compare the efficiency of laminin attachment. The polymers chosen have different chemical structures (Figure 1), ranging from the linear and simple structure of polyethylene to the aromatic-ring-containing structure of polystyrene to more complicated polymers, such as PES and PSU, that contain multiple elements. Insights into polymer properties after plasma activation, how they affect laminin attachment density and the subsequent influence of this immobilized laminin layer on cell attachment creates fundamental knowledge for future development of polymer scaffolds for islet encapsulation. The future direction of producing structured polymer scaffolds with a compound ECM can be applied more broadly to improve both islet function harvested from whole pancreas, as well as in stem-cell differentiation protocols as a novel source of transplant material.

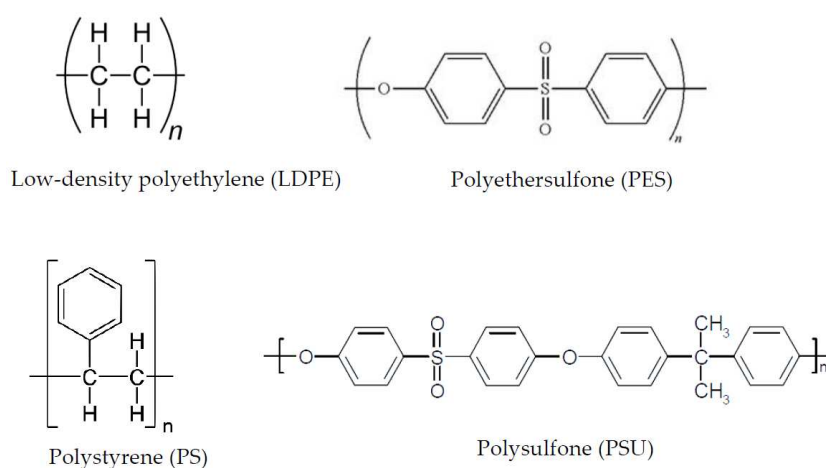


Figure 1. Molecular structure of polymers used in this paper.

2. Materials and Methods

2.1. PIII Treatment of Polymers

Polymer films of polyether sulfone (PES), polystyrene (PS), low-density polyethylene (LDPE) and polysulfone (PSU) of 0.05 mm thickness were purchased from Goodfellow Cambridge Ltd. (Huntingdon, UK). The films were treated by the PIII technique to activate their surfaces. In this technique, samples were attached on a stainless-steel sample holder with an electrically connected conducting mesh placed 5 cm in front of the holder. The sample, holder and mesh assembly were immersed in nitrogen plasma generated using inductively coupled radio frequency power at 13.56 MHz. A matching box controlled a forward power of 100 W and a reverse power of 12 W when matched. A pulse generator delivered negative bias at 20 keV in a pulsed regime to the sample holder with a pulse length of 20 μ s and a frequency of 50 Hz. The treatment was conducted for 400 s which provides a fluence of 5×10^{15} ions/cm² bombarding the sample surface. After the treatment, samples were stored in petri dishes at ambient conditions until use.

2.2. Surface Characterisation

Contact angle measurement and surface energy calculation. A theta tensiometer (Biolin Scientific, Västra Frölunda, Sweden) was used to measure contact angles of liquid probes (water and diiodomethane) on the PIII-treated and untreated polymers. Surface energy was calculated from the average of 5 contact angles using the Owens, Wendt, Rabel and Kaelble model.

Fourier Transform Infrared analysis. The surface chemistry of the polymers before and after the PIII treatment was analysed by Fourier transform infrared attenuated total reflection (FTIR-ATR) spectroscopy. Spectra of PIII-treated samples were recorded using a micro-FTIR spectrometer (Bruker, Billerica, MA, USA) and compared with the spectra of untreated polymers. For each sample, 256 scans were recorded at a resolution of 4 cm^{−1}. The spectra of the PIII-treated and untreated polymers were normalized using an intense common peak on both spectra for comparison (LDPE (1468 cm^{−1}), (PS (1492 cm^{−1}), PES and PSU (1239 cm^{−1})).

X-ray photoelectron spectroscopy (XPS) analysis. Chemical compositions of polymer surfaces before and after the PIII treatment were analysed using X-ray photoelectron spectroscopy (Thermo Scientific™ K-Alpha spectrophotometer, ThermoFisher Scientific, Waltham, MA, USA) equipped with a monochromatic Al K α X-ray source. Survey spectra were acquired within the binding energy range from 0 to 1400 eV with a resolution of 1 eV. High-resolution scans of C1s, O1s and N1s were acquired with an energy step of 0.1 eV for quantification. Data were processed using Avantage software. The spectra were charged corrected by shifting the C–C/H component of C1s to 284.8 eV.

Kinetic study of radical decay. The decay of the electron spin density of PIII-treated polymers over time was measured using an electron spin resonance (ESR) spectrometer (SpinScanX, Adani, Minsk, Belarus) with a microwave frequency of 9.35 GHz and a central magnetic field of 3330 G at room temperature. Polymer films were rolled and placed into their own quartz tube with an inner diameter of 4 mm and measured from 60 min after the PIII treatment up to 10,000 min of storage. All ESR spectra were processed using Matlab software (version R2018b).

2.3. Evaluation of Laminin Attachment on Polymers before and after the PIII Treatment

Laminin attachment on untreated and PIII-treated polymer surfaces was evaluated prior to cell adhesion. Laminin (LN511, Biolamina, Sundbyberg, Sweden) was prepared in phosphate buffer saline (PBS) with a concentration of 5 μ g/mL. PIII-treated and untreated polymers were cut into 1.2 \times 1.2 cm² samples and incubated with laminin solutions at room temperature for 1 h. Samples were subsequently washed with PBS three times (10 min each wash) and with milliQ water for 10 min. After that, they were dried overnight and analysed using a micro-FTIR spectrometer (Bruker) with 256 scans at a resolution of 4 cm^{−1}. The spectrum of the surface without laminin was subtracted from the spectrum of the relevant

polymer incubated with laminin to obtain the difference. The presence of protein was detected from the absorbance of the amide I band associated with the C–O stretch vibration ($1600\text{--}1700\text{ cm}^{-1}$) and the amide II band associated with the N–H bend and C–N stretch ($1510\text{--}1580\text{ cm}^{-1}$) vibrations. The amount of protein was calculated from the intensity of the amide I peak at 1650 cm^{-1} (A_I) and the amide II peak at 1540 cm^{-1} (A_{II}) as follows:

$$\text{Amount of protein} = \frac{A_I + A_{II}/0.47}{2 \times \text{normalization factor}} \quad (1)$$

in which normalization factor is the intensity of the chosen common peak on the spectra such as 1468 cm^{-1} on LDPE, 1492 cm^{-1} on PS and 1239 cm^{-1} on PES and PSU.

2.4. Comparison of MIN6 β -Cell Density Adhering to Untreated and PIII-Treated Polymers Coated with Laminin

Cell seeding. PIII-treated and untreated polymers were cut to size and placed at the base of individual wells in a 96-well plate (96 Well TC-Treated Polystyrene Microplates, Corning®, Corning, NY, USA). Each of the wells containing polymer were incubated with $100\text{ }\mu\text{L}$ of laminin ($5\text{ }\mu\text{g/mL}$ in PBS) overnight. Wells were washed three times with PBS, and then all residual liquid was removed by vacuum aspiration. MIN6 cells were trypsinised and seeded at a density of 3×10^4 cells per well (three replicates for each type of polymer plus three uncoated, TC-treated control wells) in $150\text{ }\mu\text{L}$ of media (DMEM supplemented with 15% FBS and 100 U/mL penicillin-streptomycin). Cells were left to incubate overnight, and then washed three times with cell media prior to imaging and metabolic assay. Brightfield images were taken on an LED/Fluorescent microscope (Zeiss-AXIO, Oberkochen, Germany) at $20\times$ and $40\times$ magnifications.

Metabolic assay. Metabolic activity was measured as a proxy for viability and attachment by an XTT colorimetric assay (Sigma Aldrich, St. Louis, MO, USA) according to the manufacturer's instructions. In brief, $50\text{ }\mu\text{L}$ of combined XTT reagent plus electron-coupling reagent were added to wells that contained cells and $100\text{ }\mu\text{L}$ of fresh media. The combined reagent mixture was also added to wells without cells (polymer and culture media only) for background measurements. The plate was incubated under normal conditions ($37\text{ }^\circ\text{C}$ and $5\%\text{ CO}_2$) for seven hours before reading the spectrophotometrical absorbance on a FLUOstar Omega microplate reader (BMG Labtech, Ortenberg, Germany). Each condition was measured in triplicate, and absorbance values were corrected for the background signal for each given polymer.

2.5. Evaluation of Function in Dispersed Primary Mouse β -Cells Cultured on Laminin Coated Surfaces

To assess the functionality of β -cells cultured on laminin-coated surfaces, Fura-2 live calcium imaging was used to examine via proxy, one of the principal components of β -cell function—glucose-stimulated insulin secretion (GSIS). In brief, in response to glucose metabolism, β -cell cytosolic calcium is elevated, triggering the release of insulin vesicles [19]. This was assayed through the use of live cytosolic calcium imaging with the ratiometric Fura-2 fluorescent indicator [20].

Islet isolation. Primary mouse islets were isolated by Liberase (Roche #05401020001, Basel, Switzerland) and collagenase (Life Technologies #17104-019, Carlsbad, CA, USA) digestion using previously established protocols [21]. C57/Bl6 mice were sacrificed by cervical dislocation, in accordance with University of Sydney animal ethics protocols (ethics approval #AEAppCatA2015-908). Isolated C57/Bl6 islets were then dispersed into primary islet cells by picking into a 15 mL tube containing serum-free RPMI media (Life Technologies #11875-093, Carlsbad, CA, USA), and centrifuged at 300 rcf . The supernatant was removed, then the islet pellet was resuspended with $200\text{ }\mu\text{L}$ TrypLE Express cell dissociation enzyme (Life Technologies #12604021, Carlsbad, CA, USA) and incubated at $37\text{ }^\circ\text{C}$ for 3 min . Following this, RPMI media supplemented with $10\%\text{ FBS}$ was added to the tube and islets were further dispersed by gentle pipetting up and down. The dispersed cells

were then plated onto laminin-coated glass coverslips and allowed to settle and recover overnight at 37 °C and 5% CO₂ in an incubator.

Fura-2 AM calcium imaging. A measure of 2 µL of 2 mM Fura-2 AM (Molecular Probes, #F1221, Eugene, OR, USA) in DMSO was complexed with 2 µL of 10% pluronic acid (Sigma-Aldrich, #P2443, St. Louis, MO, USA) in a 0.2 mL tube. This mixture was warmed to 42 °C, then dissolved in 1 mL of Krebs-Ringer bicarbonate buffer (KRB) containing 3 mM D-glucose to produce the 4 µM Fura-2 AM loading buffer. Cells were incubated with the loading buffer for 30 min at 37 °C, then washed with KRB containing 3 mM D-glucose to remove excess dye. This was then replaced with fresh KRB containing 3 mM D-glucose.

Imaging was performed using a Nikon Eclipse (Tokyo, Japan) Ti-E spinning disc confocal microscope within a dark chamber. Chamber conditions were 37 °C with 5% CO₂. Samples were excited alternately between 340 and 380 nm with a 50 milli second interval using a Lambda DG-4 Xenon lamp (Sutter Instruments, Novato, CA, USA). Basal recordings were acquired at 3 mM glucose for 3 min, then cells were stimulated with high glucose by switching the buffer to KRB containing 15 mM glucose, and recorded for 45 min.

In situ calibration of the experiments was performed by incubating samples with high Ca²⁺ (10 mM) KRB with 5 µM ionomycin (Sigma-Aldrich, #I3909, St. Louis, MO, USA), or Ca²⁺-free KRB with 5 µM ionomycin and 5 mM EGTA (Sigma-Aldrich, #E3889, St. Louis, MO, USA) to obtain R_{max} and R_{min} values, respectively. These values were then used to calculate intracellular Ca²⁺ using the Tsien formula [20], as follows:

$$[Ca^{2+}] = K_d \left(\frac{R - R_{min}}{R_{max} - R} \right) \left(\frac{S_{f2}}{S_{b2}} \right) \quad (2)$$

where: K_d is the dissociation constant of Fura-2, 225 nM [20], R is the ratio of 340 to 380 nm fluorescence at the respective timepoint, R_{min} is the minimum 340/380 nm ratio at zero calibration [Ca²⁺], R_{max} is the maximum 340/380 nm ratio at saturating calibration [Ca²⁺], S_{f2} is the 380 nm fluorescence at zero calibration [Ca²⁺] and, S_{b2} is the 380 nm fluorescence at saturating calibration [Ca²⁺].

3. Results

3.1. Surface Properties Change after the PIII Treatment

Ion bombardment from the PIII treatment has been found to induce radical formation within surfaces of polymer structures [10]. Those on the surface are oxidized when exposed to air, resulting in the appearance of polar groups which together with the remaining high energy radicals increase the hydrophilicity of the surfaces [11]. With the four polymers in this study, there were significant reductions of water contact angles from 90° on the untreated polymers to approximately half after the treatment (Figure 2A). Among all polymers, LDPE had the highest post-treatment contact angle (64°) while PSU (45°) and PES (47°) have the lowest post-treatment contact angles. The surface energy calculation shows that the polar component of the surface energy dramatically increases after the PIII treatment (Figure 2B) while the dispersive component does not change much (Figure 2C). This increased polar surface free energy is associated with the appearance of the polar groups and the unpaired electrons of radicals.

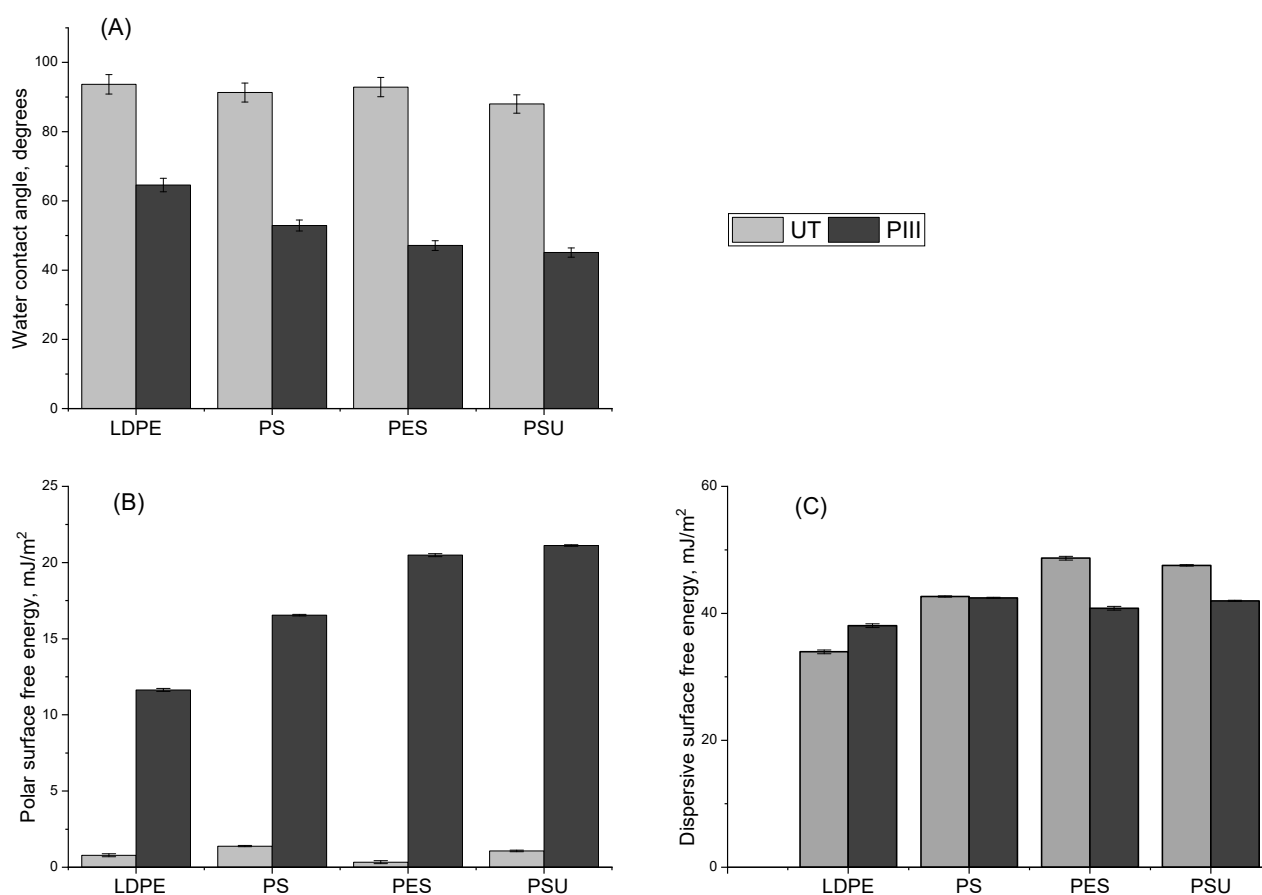


Figure 2. Comparison of surface wettability and energy between polymers before and after the PIII treatment. (A) Contact angle measurement of water, (B) polar surface energy and (C) dispersive surface energy. Light grey and dark grey denote untreated samples (UT) and PIII-treated samples (PIII), respectively. Error bars are standard deviation with $n = 5$.

The change of chemical structures of the polymer surfaces was further investigated by FTIR as shown in Figure 3. The LDPE spectrum shows the typical character of an aliphatic compound with strong C-H stretch vibrations in the range of $2950\text{--}2800\text{ cm}^{-1}$ while the other polymers show the peaks in the range of $1600\text{--}1400\text{ cm}^{-1}$ from benzene ring vibrations [22]. Compared to the spectra of the untreated polymers, the spectra of the PIII-treated polymers show a strong absorbance from the O-H stretch vibration in the range $3700\text{--}3200\text{ cm}^{-1}$. There is also absorbance in the range $1600\text{--}1800\text{ cm}^{-1}$ corresponding to C=C, C=N and C=O vibration lines, resulting from carbonisation, nitrogen ion implantation and oxidation, respectively. Compared to that in PS, the difference between untreated and PIII-treated LDPE, PSU and PES in the $1600\text{--}1800\text{ cm}^{-1}$ wavenumber range is much smaller, indicating less C=O, C=C and C=N groups forming on these polymers after the treatment.

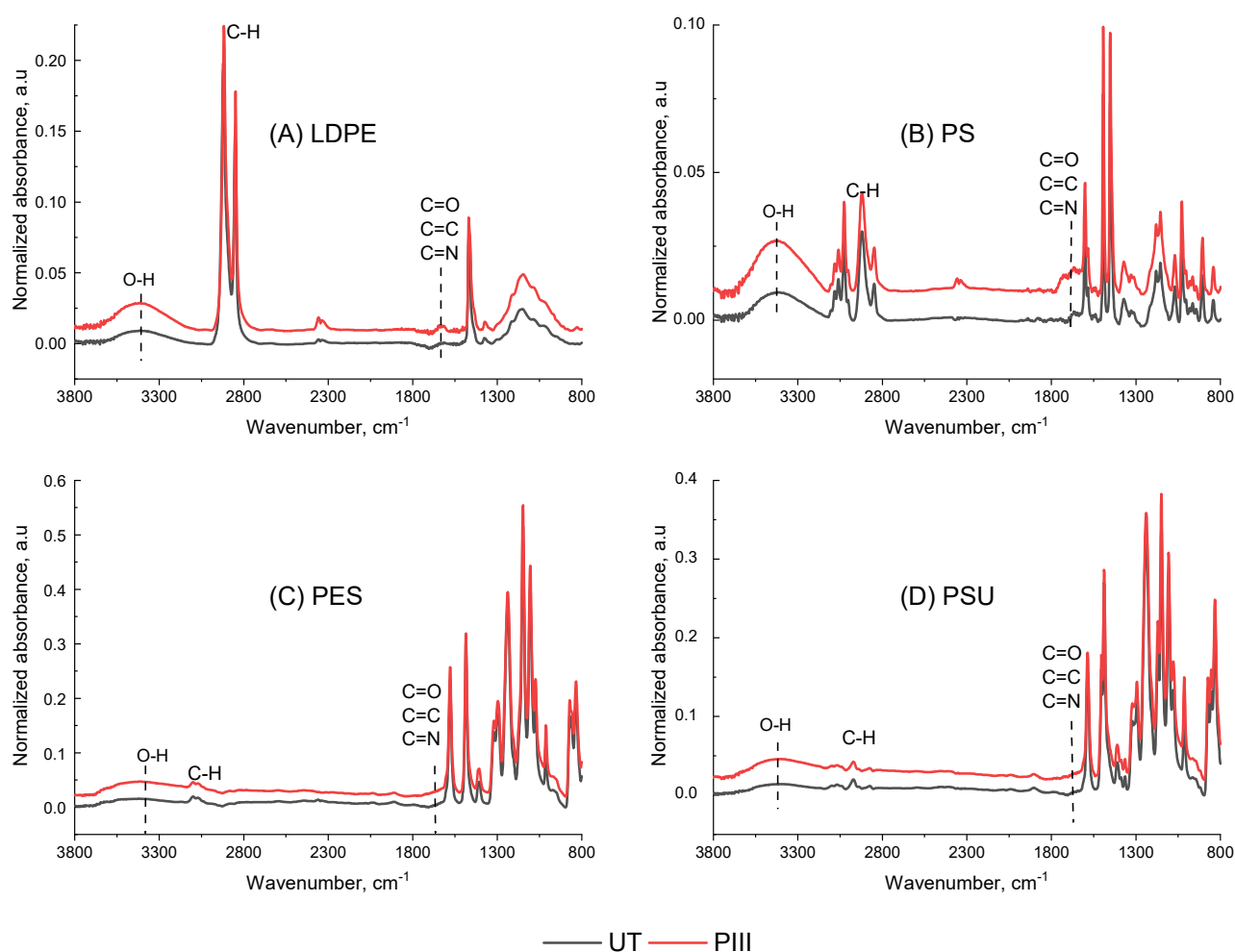


Figure 3. Comparison of FTIR-ATR spectra of the polymers before and after the PIII treatment. (A) LDPE, (B) PS, (C) PES and (D) PSU. Black and red lines represent spectra measured on untreated (UT) and PIII-treated polymers, respectively.

The change of chemical structures after the PIII treatment is more obvious from XPS analysis. High-resolution XPS scans show a change in C1s shape after the PIII treatment (Figure 4A,B) in which the peak is broadened in the high binding energy area corresponding to carbon bonds with oxygen and nitrogen. This change is more significant in PS and LDPE spectra for which the untreated polymers do not contain oxygen. An example of deconvoluted C1s peaks of PSU show that the C1s spectrum of untreated PSU (Figure 4C) consists of a major component at 284.8 eV attributed to C–C and a minor component at 286.3 eV attributed to C–O and C–S peaks. In addition, there is a π - π^* shake-up satellite from aromatic rings at 291.4 eV, accounting for 2.6% of the C1s peak area. After the treatment, two new components appear at 287.8 and 289.2 eV corresponding to C=O, C=N and O–C=O peaks, respectively (Figure 4D). The π - π^* satellite reduces to 1.3% of the overall C1s area, indicating that the ion bombardment greatly influences the conjugated system of aromatic rings.

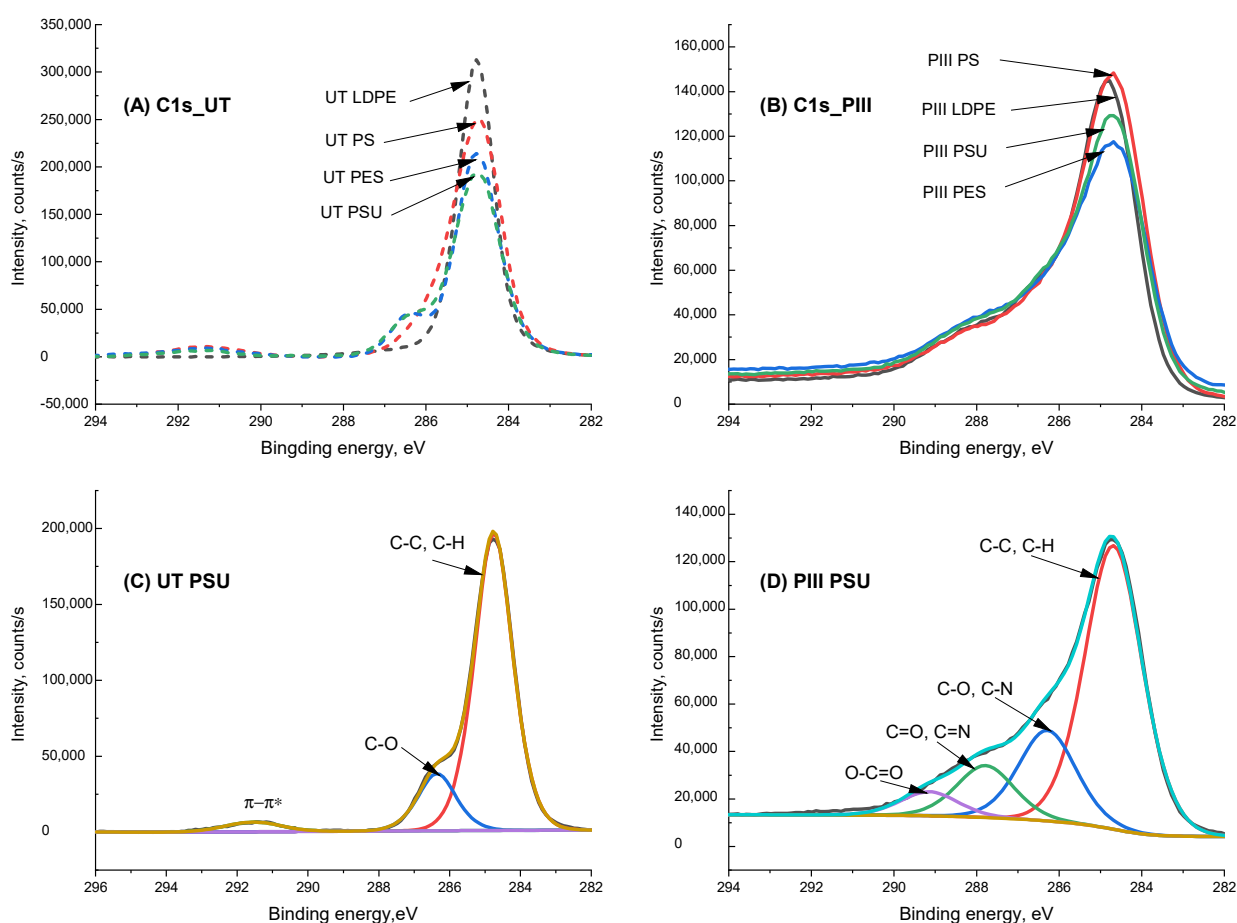


Figure 4. XPS C1s carbon peak. Comparison of the C1s peak of the 4 polymers before (A) and after the PIII treatment (B). Deconvoluted C1s peak of untreated PSU (C) and PIII-treated PSU (D). Dashed lines and solid lines represent untreated and PIII-treated polymer spectra, respectively.

Composition analysis (Table 1) shows a significant increase of nitrogen and oxygen on all polymers after the PIII treatment. Figure 5A compares O1s peaks of four untreated polymers. As predicted from polymer molecular structure, no oxygen is detected on LDPE and PS. On these polymers, the oxygen content increases 16%–17% after PIII treatment while it only slightly increases (approximately 2%) on the oxygen-containing polymers (PES and PSU). O1s peaks on untreated PES and PSU can be deconvoluted into two components at 531.7 and 533.2 eV which can be assigned to O=S=O and C–O groups, respectively [23,24]. After the PIII treatment, the O1s peaks of all the polymers have the same shape and similar intensity (Figure 5B) in which the main component (>90%) is at approximately 531.7 eV which is assigned to C=O and/or O=S=O. N1s peaks are not detected on untreated polymers but appear on all polymers (8%–9%) after the treatment with approximately the same shape and intensity (Figure 5C). Overall, the shapes of C1s, O1s and N1s detected on all of the PIII-treated polymers are very similar despite their differences before the treatment. The S2p peaks of PSE and PSU are reduced after the PIII treatment with a shift to the lower binding energy area (Figure 5D). Untreated PES and PSU have S2p peaks that appear at high binding energy (>166 eV) correlated to oxidized sulphur (C–SO₂–C) while PIII-treated PES and PSU have a ratio of 20% remaining in high binding energy area and there was an 80% shift to a lower energy (peaks at 163 eV) correlating to sulphide groups (C–S–C). This means that sulfone groups were not oxidized into SO₄ groups (which appear in higher binding energy) but rather that oxygen molecules were knocked off sulfone groups as a result of ion bombardment. Compared to UV radiation on PES [12], which reduces the water contact angle to 40°, increases the oxygen content

(from 20.0 ± 0.8 to 28.6 ± 1.0) and slightly changes the sulphur content (from $5.5\% \pm 0.2\%$ to $5.6\% \pm 0.2\%$) and nitrogen content (from $0.2\% \pm 0.2\%$ to $2.4\% \pm 0.7\%$), the PIII treated PES has approximately the same hydrophilicity but lower oxygen and sulphur and higher nitrogen content. It can be inferred that there are fewer oxygen-containing groups and more nitrogen-containing groups on the PIII-treated PES; therefore, the surface has higher positive charge than the UV-treated PES.

Table 1. Atomic percentages of elements detected on polymer surfaces using XPS.

Sample	C1s	N1s	O1s	S2p
LDPE	99.6	0.0	0.4	-
PIII LDPE	73.5	8.9	17.6	-
UT PS	99.3	0.0	0.8	-
PIII PS	75.4	8.5	16.1	-
UT PES	75.5	0.0	18.3	6.2
PIII PES	67.0	8.5	20.4	4.1
UT PSU	78.4	0.6	17.9	3.1
PIII PSU	69.3	9.2	19.4	2.1

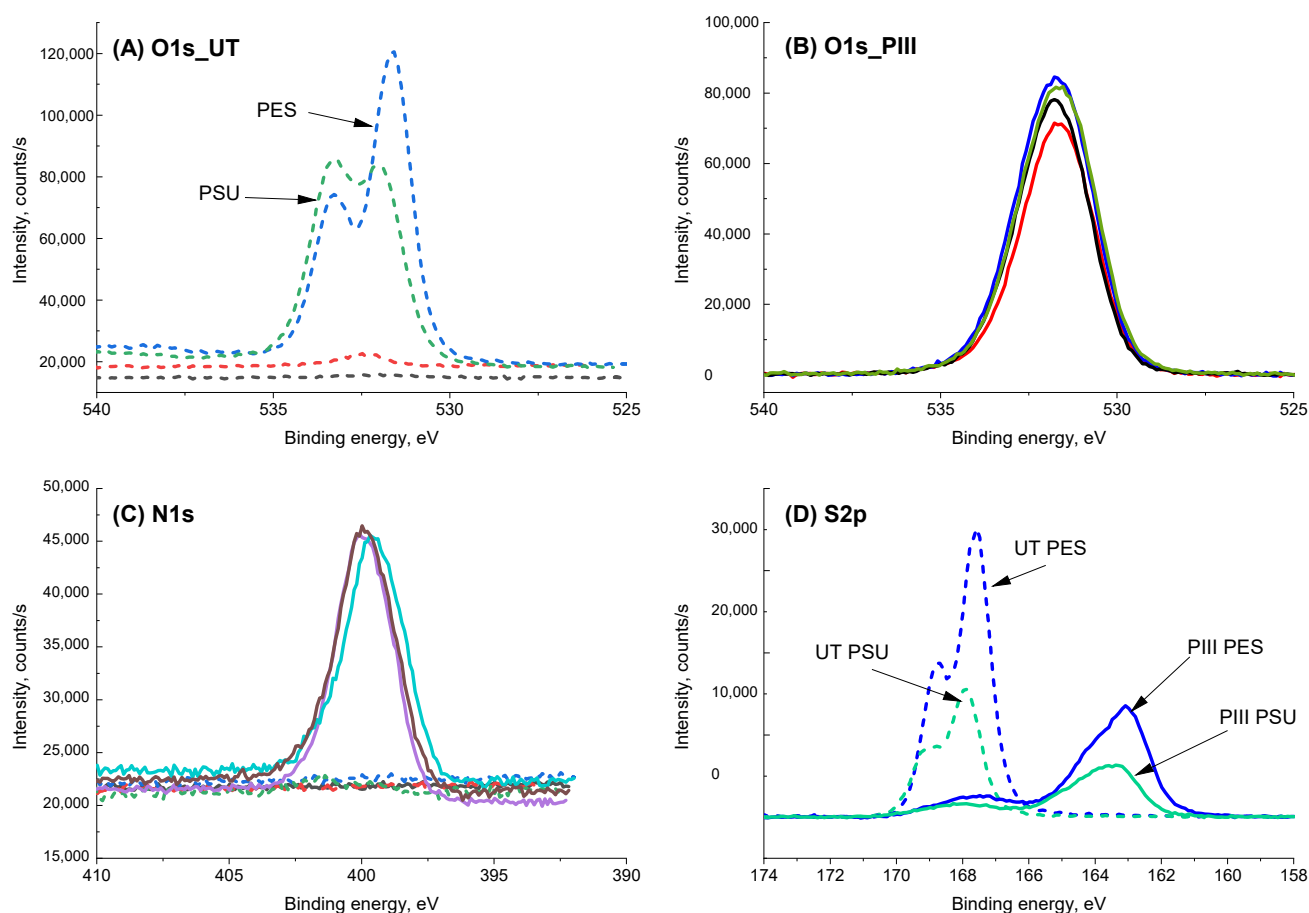


Figure 5. Comparison of XPS high-resolution scans. O1s peak of the 4 polymers before (A) and after (B) the PIII treatment. N1s peaks of the 4 polymers before and after the PIII treatment (C). S2p peaks of PES and PSU before and after the PIII treatment (D). Dashed lines and solid lines represent untreated and PIII-treated polymers, respectively.

Radical decay on PIII-treated samples stored under ambient conditions was studied by measuring ESR for a week. ESR analysis (Figure 6) detected radicals on all four types of polymer films after the PIII treatment. The plot shows a sharp decrease within the first day of storage and more gradual decreases thereafter. Under the same conditions of treatment, the radical density measured just after the treatment on PSU is approximately three times higher than radical density detected on LDPE. Radical contents of all polymers equilibrate after about 1 week. There are comparable radical densities on PSU, PES and PS after one week and thereafter while radical density on LDPE remains the lowest. This result is consistent with the low polar surface energy calculated on the PIII-treated LDPE. The difference of radical density can be explained by the original chemical structure of the polymers. When ion bombardment occurs during the PIII treatment, polymer chains on the surface are fragmented and ion tracks penetrate deep into the bulk polymer, creating tracks containing high radical content [11]. Radical reactions induce cross linking of polymer chains. Kosobrodova et al. [25] found that when the ion fluence exceeds 10^{13} ions/cm², carbonized clusters appear in the polymer surface. The number of clusters and the cluster size increase with the level of ion bombardment. It is known that the unpaired electrons of radicals are stabilized by delocalisation associated with π bonds [26]. It is the carbonized structure forming due to ion bombardment that protects and stabilizes free radicals from being more rapidly quenched. Among the four polymers studied, PS, PES and PSU have aromatic rings in their structures; therefore, the number and size of carbonized clusters forming on these polymers are expected to be higher than on LDPE, resulting in higher radical density with the same conditions of PIII treatment.

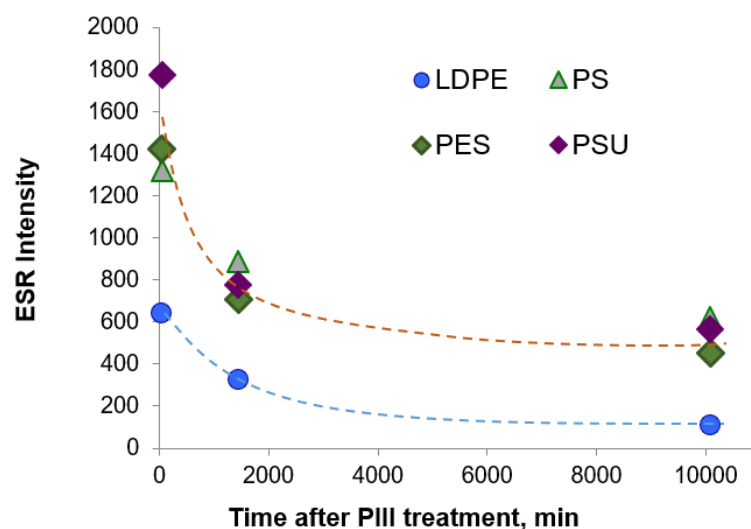


Figure 6. Radical decay on PIII-treated polymers during storage at ambient conditions for the first 7 days after the treatment.

3.2. Laminin Attachment on Untreated and PIII-Treated Polymers

Previous works have demonstrated covalent attachment of biomolecules on the PIII-treated surface as opposed to physical adsorption on untreated polyethylene [27], polyethersulfone [28] and polystyrene [29,30]. These differences in surface attachment of the biomolecules have been revealed using stringent washing with detergent at high temperatures. In this work, we are interested in comparing the laminin density attached on both surfaces which subsequently influences cell adhesion.

Laminin was immobilized on the untreated and PIII-treated polymers and analysed by FTIR spectroscopy for comparison. Protein signals were detected at significantly higher levels on the PIII-treated surfaces compared to the untreated surfaces, except for the case of LDPE, where the difference was not significant (Figure 7). Surface wettability and radical density are among the factors influencing the protein attachment in this experiment. Hydrophobic surfaces of untreated polymers can induce protein molecules to expose hy-

drophobic domains, resulting in conformation change when the protein is adsorbed on the surface while the hydrophilic surfaces of PIII-treated polymers with a water contact angle between 50° and 60° is ideal for protein adsorption without changing its conformation. Radicals provide binding sites for the adsorbed molecules to covalently attach to the surface and therefore resist the shear force during the washing steps. In terms of radical density, this laminin attachment experiment was conducted two months after the PIII treatment when the radical density on all polymers is in the relatively stable part of the ESR curve. According to the ESR results (Figure 6), LDPE has the lowest radical density, which explains why the normalized signal of laminin immobilized on the PIII-treated LDPE is only slightly higher than that on the untreated LDPE.

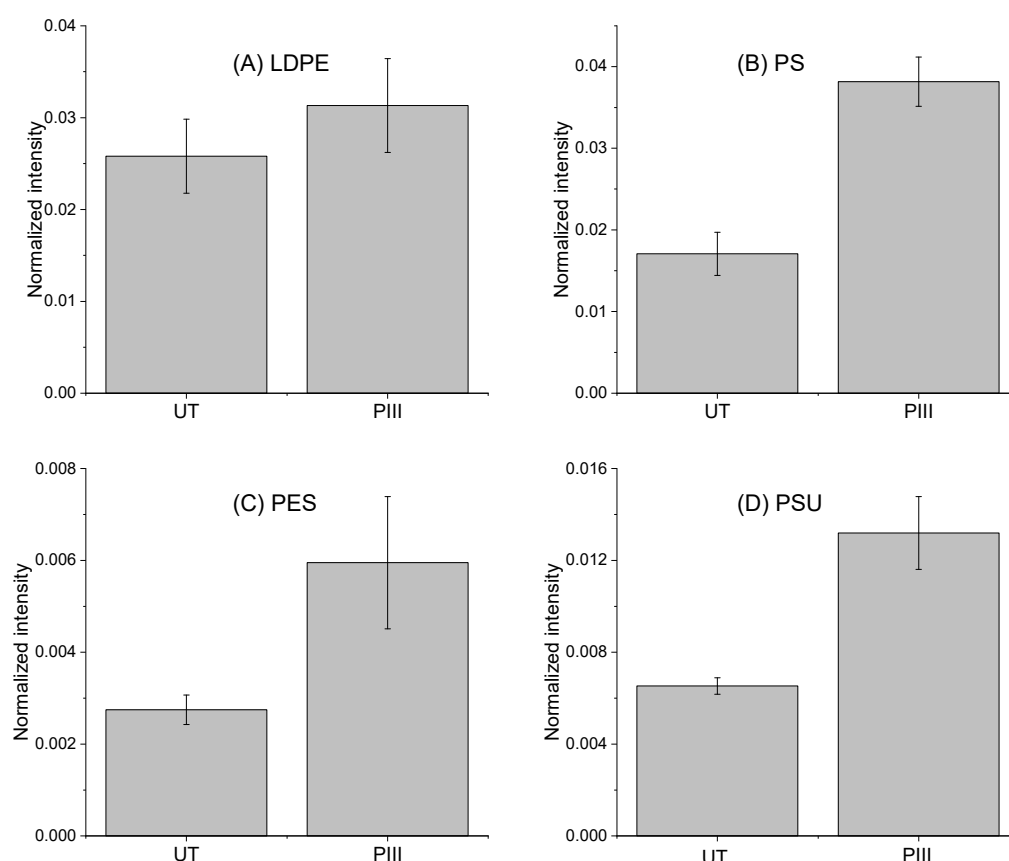


Figure 7. Comparison of protein intensity calculated from amide I and amide II peaks of FTIR spectra of untreated (UT) and PIII-treated (PIII) polymers: (A) LDPE; (B) PS; (C) PES and (D) PSU.

3.3. MIN6 β -Cell Attachment on Untreated and PIII-Treated Surfaces

Figure 8 shows MIN6 cell distributions on untreated and PIII-treated polymers coated with laminin at two different magnifications. On the untreated polymers, MIN6 cells sparsely adhered to the surface with large aggregations and spaces in between. This could be due to the non-uniform distribution or the denaturation of laminin molecules on the untreated polymer surfaces. In contrast, MIN6 cells attached on the PIII-treated surfaces with higher density and more regular distribution. XTT colorimetric assays (Figure 9) confirmed that cell density on PIII-treated surfaces is significantly higher than that on untreated surfaces ($p < 0.05$) except for in the case of LDPE. PIII-treated PS, PES and PSU have higher values than that for the tissue culture-treated well but not statistically significant at the level of 0.05 confidence.

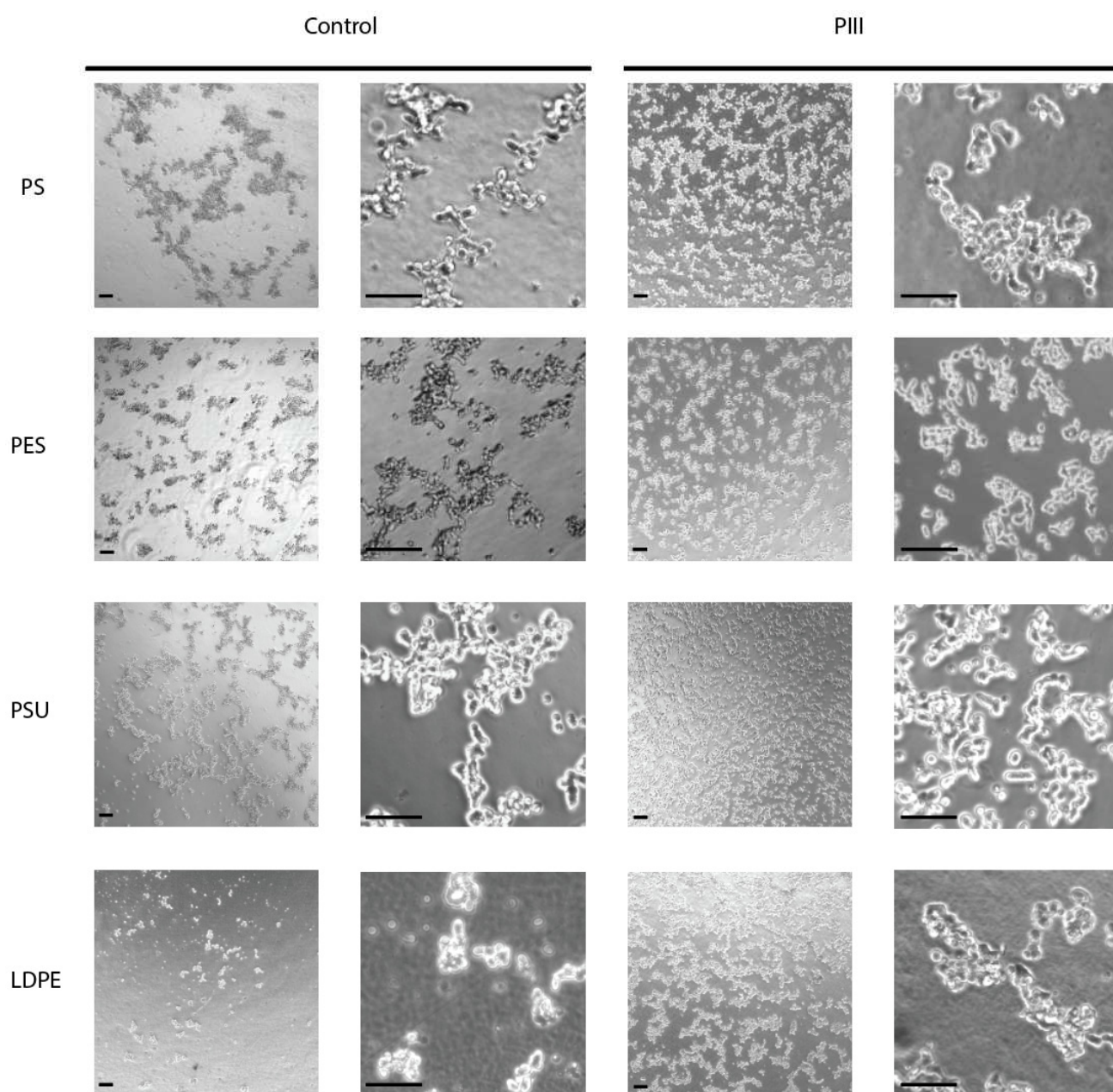


Figure 8. MIN6 cells were seeded on PIII-treated and untreated polymers coated with laminin. Brightfield images were taken on a fluorescent desktop microscope at 20× and 40× magnification. Scale bar represents 50 μm.

To study the functionality of the β -cells cultured on laminin 511, we immobilized laminin on glass cover slips and used Fura-2 calcium imaging to examine the glucose-induced calcium response. This study was conducted on glass cover slips due to their high transparency for optical microscopy which polymers cannot meet. Previous work has shown that the archetypal oscillatory glucose-induced calcium phenotype is lost upon dispersion of whole islets into single β -cells [31,32], with loss of gap junctional connections suggested to be responsible [33]. However, the exemplar calibrated calcium trace in Figure 10 demonstrates an oscillatory calcium response in dispersed β -cells, resembling the signature of intact islets. This improvement may be attributed to the formation of focal adhesion complexes at the point of cell–ECM contact, as has been previously reported [18]. Although this assay of β -cells functionality on laminin was not directly conducted on the PIII-treated polymers, this observation provides positive evidence for the monolayer cul-

ture of β -cells within the context of polymer scaffolds with PIII-immobilised ECM proteins.

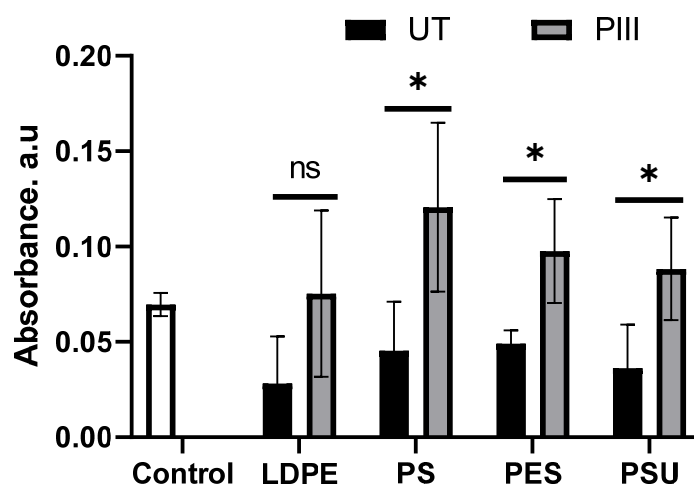


Figure 9. Comparison of MIN6 β -cell adhesion on untreated and PIII-treated polymers coated with laminin from XTT calorimetric assays. Control wells are standard tissue-culture 96-well plate. Error bars were calculated from three replicates. The differences between UT and PIII-treated samples were analysed using unpaired *t*-tests with statistically significant differences shown as * $p < 0.05$ ($n = 3$).

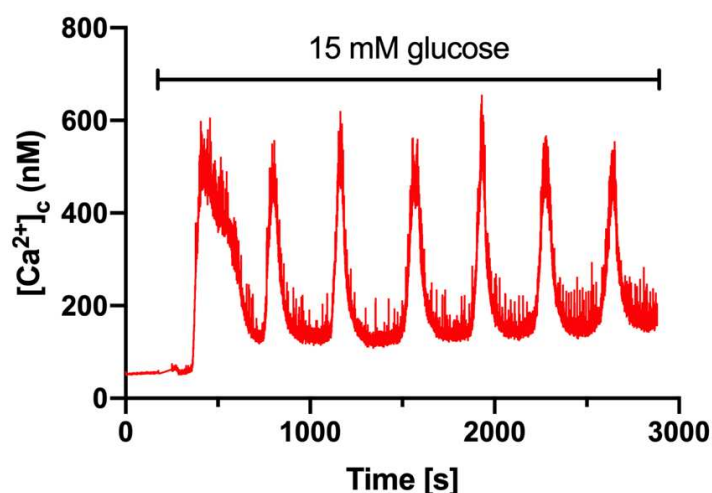


Figure 10. Primary mouse β -cells display the archetypal glucose-induced oscillatory calcium phenotype when cultured on laminin. Exemplar trace demonstrates robust cytosolic calcium oscillations in primary mouse β -cells in response to 15 mM glucose stimulation.

While further studies are needed to examine the β -cell survival and functionality in the microencapsulation environment, our results show promising cell attachment on the PIII-treated polymers coated with laminin. Taken together with previous work that showed that covalently attached IL4 on PIII-treated PES membranes mitigated the local foreign body response [1,28], our work suggests a polymer membrane capsule design. A PIII-treated polymer membrane capsule would enable facile covalent immobilisation of a basal membrane adhesion molecule, such as laminin, on the capsule's inner surface to promote β -cell function, whilst facilitating IL-4 immobilisation on the outside to mitigate fibrosis. Covalent attachment of the functional bioactive molecules is necessary to prevent their loss through protein exchange, such as via the Vroman effect [34]. Compared to the immobilization of laminin-derived peptides on poly (caprolactone) using a chemical linker [8] or on fluorinated ethylene propylene using glow discharge and chemical reaction [35] which require multiple steps, PIII-treatment provides a simple, reagent-free

approach, facilitated by reactions with surface embedded radicals, to enable patterned covalent immobilisation of the functional biomolecules onto the membrane surfaces. In this study, despite similar changes of surface wettability and surface chemistry, three out of four candidate polymers were identified as prospective for the development of such β -cell encapsulation structures due to their capability to form and preserve radicals after the ion implantation treatment. The immobilisation of the proteins on the activated surfaces, as shown in this work as well as in previous work [1], is very straightforward in PBS buffer solution without any further surface modification or additional chemicals.

4. Conclusions

We have demonstrated that the PIII treatment of four types of polymers (LDPE, PS, PES and PSU) changes their surface properties and improves laminin attachment density. The chemistry changes include the forming of oxygen containing groups and radicals, which increases the polar surface energy and hydrophilicity of the polymers. Despite the difference in chemical structure, the surface properties of all investigated polymers after the PIII treatment are quite similar from XPS surface component analysis (C, N and O). Among the four polymers, LDPE has the lowest radical density after the treatment and shows no significant improvement in laminin attachment and MIN6 β -cell adhesion after 2 months. PIII-treated PS, PES and PSU bind laminin with higher density than the untreated surfaces, resulting in better MIN6 β -cell adhesion which is comparable to that on the commercial tissue culture plate. Finally, it was shown that culturing β -cells in monolayers on immobilised laminin restored their functionality to that of intact islets. The knowledge gained from PIII treatment of polymers in this research will provide good guidance for selecting polymer membrane candidates for β -cell encapsulation and other fields in which the optimisation of surface–protein interactions is important.

Author Contributions: Conceptualization, M.B., P.T. and E.K.; methodology, E.K., J.T., N.H. and C.T.; investigation, E.K., J.T., N.H. and C.T.; writing—original draft preparation, C.T., J.T. and N.H.; writing—review and editing, M.B., P.T., J.T., N.H. and C.T. All authors have read and agreed to the published version of the manuscript.

Funding: This research was funded by the Australian Research Council (ARC), Grant Nos. FT12010 0226; DP130103693; FL190100216; DP190103507 and the NHMRC Grant Nos APP1128273 and APP1146788.

Institutional Review Board Statement: The study was performed in accordance with animal ethical procedures approved by the University of Sydney Research Integrity and Ethics Administration Committee (project #908, 2015).

Informed Consent Statement: Not applicable.

Data Availability Statement: Data can be provided upon request.

Acknowledgments: The authors acknowledge the facilities and technical assistance of the Australian Microscopy & Microanalysis Research Facility and Sydney Analytical Core Facility at the University of Sydney.

Conflicts of Interest: The authors declare no conflict of interest.

References

1. Tan, R.P.; Hallahan, N.; Kosobrodova, E.; Michael, P.L.; Wei, F.; Santos, M.; Lam, Y.T.; Chan, A.H.P.; Xiao, Y.; Bilek, M.M.M.; et al. Bioactivation of encapsulation membranes reduces fibrosis and enhances cell survival. *ACS Appl. Mater. Interfaces* **2020**, *12*, 56908–56923. [[CrossRef](#)]
2. Kragl, M.; Lammert, E. Basement membrane in pancreatic islet function. *Adv. Exp. Med. Biol.* **2010**, *654*, 217–234. [[CrossRef](#)]
3. Weber, L.M.; Hayda, K.N.; Anseth, K.S. Cell-matrix interactions improve beta-cell survival and insulin secretion in three-dimensional culture. *Tissue Eng. Part A* **2008**, *14*, 1959–1968. [[CrossRef](#)]
4. Otonkoski, T.; Banerjee, M.; Korsgren, O.; Thornell, L.E.; Virtanen, I. Unique basement membrane structure of human pancreatic islets: Implications for beta-cell growth and differentiation. *Diabetes Obes. Metab.* **2008**, *10* (Suppl. 4), 119–127. [[CrossRef](#)] [[PubMed](#)]

5. Virtanen, I.; Banerjee, M.; Palgi, J.; Korsgren, O.; Lukinius, A.; Thornell, L.E.; Kikkawa, Y.; Sekiguchi, K.; Hukkanen, M.; Kontinen, Y.T.; et al. Blood vessels of human islets of Langerhans are surrounded by a double basement membrane. *Diabetologia* **2008**, *51*, 1181–1191. [CrossRef] [PubMed]
6. Desai, S.M.; Singh, R.P. Surface modification of polyethylene. In *Long Term Properties of Polyolefins*; Albertsson, A.-C., Ed.; Springer: Berlin/Heidelberg, Germany, 2004; pp. 231–294.
7. Singh, R.K.; Jin, G.-Z.; Mahapatra, C.; Patel, K.D.; Chrzanowski, W.; Kim, H.-W. Mesoporous silica-layered biopolymer hybrid nanofibrous scaffold: A novel nanobiomatrix platform for therapeutics delivery and bone regeneration. *ACS Appl. Mater. Interfaces* **2015**, *7*, 8088–8098. [CrossRef] [PubMed]
8. Santiago, L.Y.; Nowak, R.W.; Peter Rubin, J.; Marra, K.G. Peptide-surface modification of poly(caprolactone) with laminin-derived sequences for adipose-derived stem cell applications. *Biomaterials* **2006**, *27*, 2962–2969. [CrossRef]
9. Bilek, M.; McKenzie, D. Plasma modified surfaces for covalent immobilization of functional biomolecules in the absence of chemical linkers: Towards better biosensors and a new generation of medical implants. *Biophys. Rev.* **2010**, *2*, 55–65. [CrossRef] [PubMed]
10. Kosobrodova, E.A.; Kondyurin, A.V.; Fisher, K.; Moeller, W.; McKenzie, D.R.; Bilek, M.M.M. Free radical kinetics in a plasma immersion ion implanted polystyrene: Theory and experiment. *Nucl. Instrum. Methods Phys. Res. Sect. B* **2012**, *280*, 26–35. [CrossRef]
11. Kondyurin, A.; Bilek, M. *Ion Beam Treatment of Polymers*; Elsevier: Amsterdam, The Netherlands, 2008.
12. Cisse, I.; Oakes, S.; Sachdev, S.; Toro, M.; Lutondo, S.; Shedden, D.; Atkinson, K.M.; Shertok, J.; Mehan, M.; Gupta, S.K.; et al. Surface modification of polyethersulfone (PES) with UV photo-oxidation. *Technologies* **2021**, *9*, 36. [CrossRef]
13. Yousif, E.; Hasan, A. Photostabilization of poly(vinyl chloride)—Still on the run. *J. Taibah Univ. Sci.* **2015**, *9*, 421–448. [CrossRef]
14. Tran, C.T.; Nosworthy, N.J.; Kondyurin, A.; McKenzie, D.R.; Bilek, M.M. CelB and β -glucosidase immobilization for carboxymethyl cellulose hydrolysis. *RSC Adv.* **2013**, *3*, 23604–23611. [CrossRef]
15. Bax, D.V.; Wang, Y.; Li, Z.; Maitz, P.K.M.; McKenzie, D.R.; Bilek, M.M.M.; Weiss, A.S. Binding of the cell adhesive protein tropoelastin to PTFE through plasma immersion ion implantation treatment. *Biomaterials* **2011**, *32*, 5100–5111. [CrossRef]
16. Tran, C.T.H.; Craggs, M.; Smith, L.M.; Stanley, K.; Kondyurin, A.; Bilek, M.M.; McKenzie, D.R. Covalent linker-free immobilization of conjugatable oligonucleotides on polypropylene surfaces. *RSC Adv.* **2016**, *6*, 83328–83336. [CrossRef]
17. Drobeta, M.; Aflori, M.; Gradinaru, L.M.; Coroaba, A.; Butnaru, M.; Vlad, S.; Vasilescu, D.S. Collagen immobilization on ultraviolet light-treated poly(ethylene terephthalate). *High Perform. Polym.* **2015**, *27*, 646–654. [CrossRef]
18. Gan, W.J.; Do, O.H.; Cottle, L.; Ma, W.; Kosobrodova, E.; Cooper-White, J.; Bilek, M.; Thorn, P. Local integrin activation in pancreatic β cells targets insulin secretion to the vasculature. *Cell Rep.* **2018**, *24*, 2819–2826.e3. [CrossRef] [PubMed]
19. Henquin, J.-C. The dual control of insulin secretion by glucose involves triggering and amplifying pathways in β -cells. *Diabetes Res. Clin. Pract.* **2011**, *93*, S27–S31. [CrossRef]
20. Grynkiewicz, G.; Poenie, M.; Tsien, R.Y. A new generation of Ca^{2+} indicators with greatly improved fluorescence properties. *J. Biol. Chem.* **1985**, *260*, 3440–3450. [CrossRef]
21. Do, O.H.; Low, J.T.; Thorn, P. Lepr(db) mouse model of type 2 diabetes: Pancreatic islet isolation and live-cell 2-photon imaging of intact islets. *Journal of visualized experiments. JoVE* **2015**, *99*, e52632. [CrossRef]
22. Alenazi, N.A.; Hussein, M.A.; Alamry, K.A.; Asiri, A.M. Nanocomposite-based aminated polyethersulfone and carboxylate activated carbon for environmental application. A Real Sample Analysis. C—J. *Caron Res.* **2018**, *4*, 30. [CrossRef]
23. Liu, S.X.; Kim, J.-T. Characterization of surface modification of polyethersulfone membrane. *J. Adhes. Sci. Technol.* **2011**, *25*, 193–212. [CrossRef]
24. Wavhal, D.S.; Fisher, E.R. Membrane surface modification by plasma-induced polymerization of acrylamide for improved surface properties and reduced protein fouling. *Langmuir* **2003**, *19*, 79–85. [CrossRef]
25. Kosobrodova, E.; Kondyurin, A.; McKenzie, D.R.; Bilek, M.M.M. Kinetics of post-treatment structural transformations of nitrogen plasma ion immersion implanted polystyrene. *Nucl. Instrum. Methods Phys. Res. Sect. B* **2013**, *304*, 57–66. [CrossRef]
26. Ashenhurst, J. 3 Factors That Stabilize Free Radicals. Available online: <https://www.masterorganicchemistry.com/2013/08/02/3-factors-that-stabilize-free-radicals/> (accessed on 15 July 2021).
27. Kondyurin, A.V.; Naseri, P.; Tilley, J.M.R.; Nosworthy, N.J.; Bilek, M.M.M.; McKenzie, D.R. Mechanisms for covalent immobilization of horseradish peroxi-dase on ion beam treated polyethylene. *Scientifica* **2011**, arXiv:1110.3125.
28. Kosobrodova, E.; Kondyurin, A.; Solodko, V.; Weiss, A.S.; McKenzie, D.R.; Bilek, M.M.M. Covalent biofunctionalization of the inner surfaces of a hollow-fiber capillary bundle using packed-bed plasma ion implantation. *ACS Appl. Mater. Interfaces* **2020**, *12*, 32163–32174. [CrossRef]
29. MacDonald, C.; Morrow, R.; Weiss, A.S.; Bilek, M.M.M. Covalent attachment of functional protein to polymer surfaces: A novel one-step dry process. *J. R. Soc. Interface* **2008**, *5*, 663–669. [CrossRef]
30. Hirsh, S.L.; Bilek, M.M.M.; Nosworthy, N.J.; Kondyurin, A.; Dos Remedios, C.G.; McKenzie, D.R. A comparison of covalent immobilization and physical adsorption of a cellulase enzyme mixture. *Langmuir* **2010**, *26*, 14380–14388. [CrossRef]
31. MacDonald, P.E.; Rorsman, P. Oscillations, intercellular coupling, and insulin secretion in pancreatic β cells. *PLoS Biol.* **2006**, *4*, e49. [CrossRef]
32. Rorsman, P.; Trube, G. Calcium and delayed potassium currents in mouse pancreatic beta-cells under voltage-clamp conditions. *J. Physiol.* **1986**, *374*, 531–550. [CrossRef]

33. Ravier, M.A.; Güldenagel, M.; Charollais, A.; Gjinovci, A.; Caille, D.; Söhl, G.; Wollheim, C.B.; Willecke, K.; Henquin, J.-C.; Meda, P. Loss of connexin36 channels alters β -cell coupling, islet synchronization of glucose-induced Ca^{2+} and insulin oscillations, and basal insulin release. *Diabetes* **2005**, *54*, 1798–1807. [[CrossRef](#)] [[PubMed](#)]
34. Hirsh, S.L.; McKenzie, D.R.; Nosworthy, N.J.; Denman, J.A.; Sezerman, O.U.; Bilek, M.M.M. The Vroman effect: Competitive protein exchange with dynamic multilayer protein aggregates. *Colloids Surf. B* **2013**, *103*, 395–404. [[CrossRef](#)]
35. Ranieri, J.P.; Bellamkonda, R.; Bekos, E.J.; Vargo, T.G.; Gardella, J.A., Jr.; Aebischer, P. Neuronal cell attachment to fluorinated ethylene propylene films with covalently immobilized laminin oligopeptides YIGSR and IKVAV. II. *J. Biomed. Mater. Res.* **1995**, *29*, 779–785. [[CrossRef](#)]